

## Supplementary Information

### In Operando Synchrotron X-ray Studies of a Novel Spinel $(\text{Ni}_{0.2}\text{Co}_{0.2}\text{Mn}_{0.2}\text{Fe}_{0.2}\text{Ti}_{0.2})_3\text{O}_4$ High-Entropy Oxide for Energy Storage Applications

Tsung-Yi Chen,<sup>1,2†</sup> Syuan-Yu Wang,<sup>1,2†</sup> Chun-Han Kuo,<sup>1,2</sup> Shao-Chu Huang,<sup>1</sup> Ming-Hsien Lin,<sup>3</sup> Chih-Heng Li,<sup>1,2,4</sup> Hsin-Yi Chen,<sup>4</sup> Chun-Chieh Wang,<sup>5,2</sup> Yen-Fa Liao,<sup>5</sup> Chia-Ching Lin,<sup>1</sup> Yu-Ming Chang,<sup>1</sup> Jien-Wei Yeh,<sup>1, 2</sup> Su-Jien Lin,<sup>1,2</sup> Tsan-Yao Chen,<sup>4</sup> Han-Yi Chen<sup>1,2\*</sup>

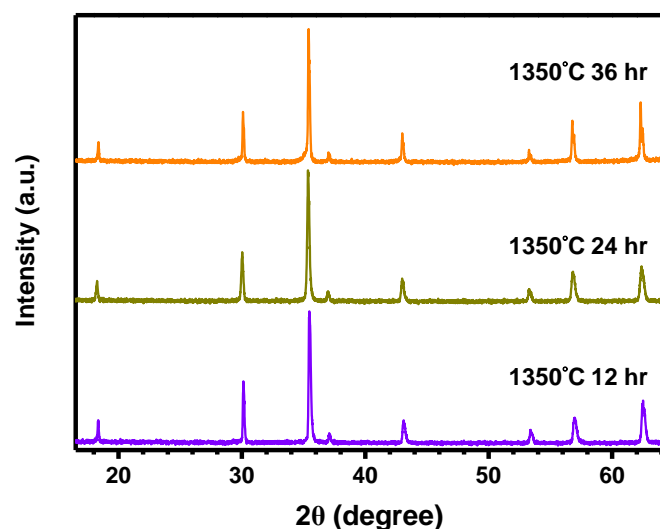


Figure S1. Enlarged XRD patterns of NCMFT at different sintering times.

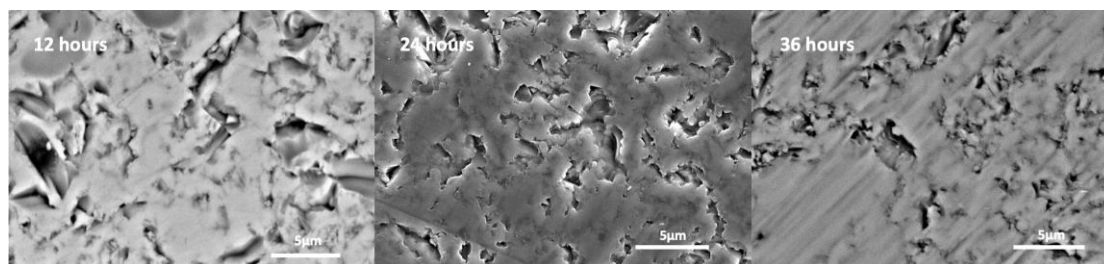


Figure S2. Backscattered Electron Image of NCMFT at different holding temperature time. From left to right, increasing holding time result in increasing homogeneity.

Table S1. Rietveld refinement parameters of NCMFT

	$(\text{Ni}_{0.2}\text{Co}_{0.2}\text{Mn}_{0.2}\text{Fe}_{0.2}\text{Ti}_{0.2})_3\text{O}_4$
Lattice	Cubic
Space group	Fd-3m
a (Å)	8.440
Rwp	9.9
GOF	1.12

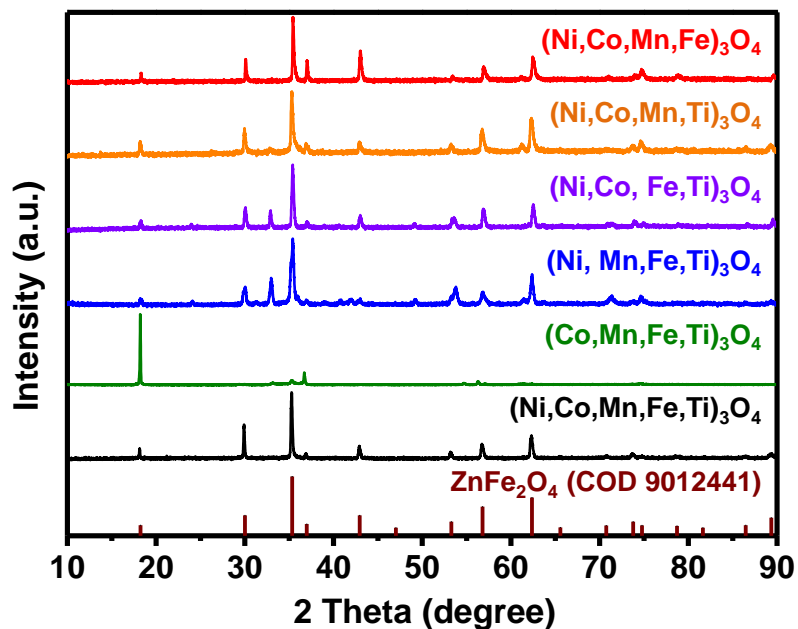


Figure S3. XRD patterns of NCMFT and quaternary oxides

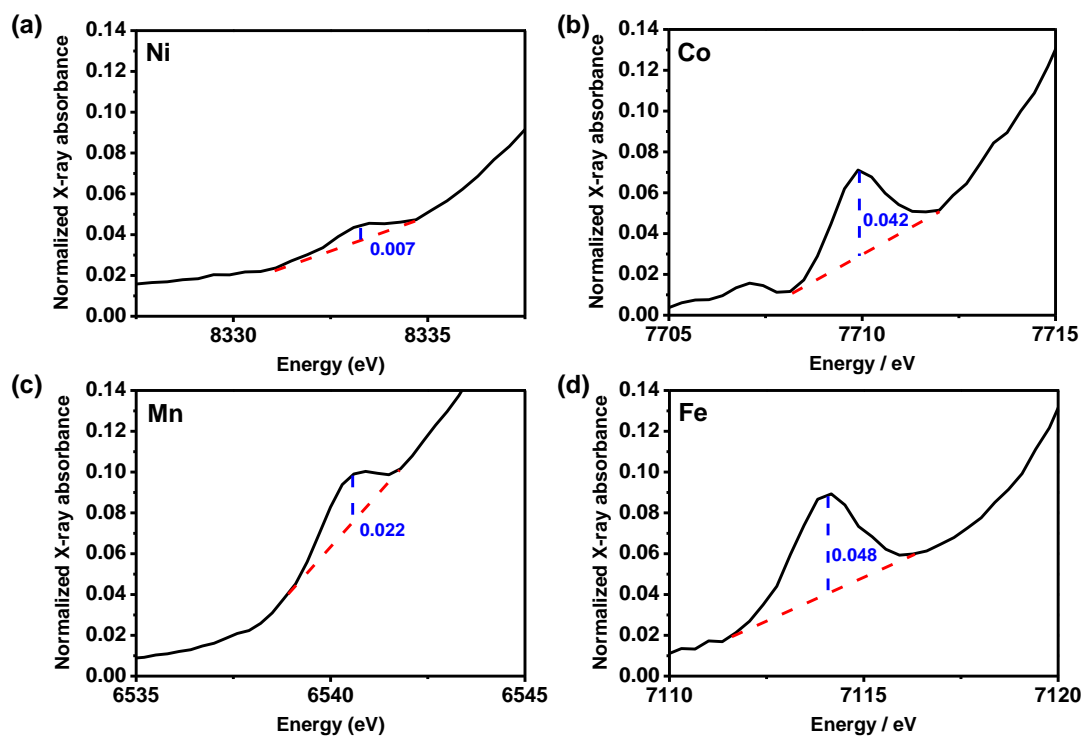


Figure S4. Enlarged XANES of NCMFT in the pre-edge part: (a) Ni K-edge; (b) Co K-edge; (c) Mn K-edge; (d) Fe K-edge.

**Table S2.** Comparison of the LIB anode performance of NCMFT with other conversion-type spinel anodes in the literature

Electrodes	Current density	1 <sup>st</sup> / 2 <sup>nd</sup> discharge capacity (mA h g <sup>-1</sup> )	Cycle No. (retention)	Rate performance	Ref.
Mn <sub>3</sub> O <sub>4</sub>	40 mA g <sup>-1</sup>	1350/300	10 <sup>th</sup> (~33%)	-	1
Co <sub>3</sub> O <sub>4</sub>	50 mA g <sup>-1</sup>	1105/817	30 <sup>th</sup> (~23%)	50 mA h g <sup>-1</sup> @ 0.5 A g <sup>-1</sup>	2
MnFe <sub>2</sub> O <sub>4</sub>	0.1C	1405/1050	10 <sup>th</sup> (~48%)	200 mA h g <sup>-1</sup> @ 0.5C	3
NiFe <sub>2</sub> O <sub>4</sub>	100 mA g <sup>-1</sup>	1100/800	100 <sup>th</sup> (~25%)	-	4
NiFeMnO <sub>4</sub>	91.8 mA g <sup>-1</sup>	1427/1100	50 <sup>th</sup> (~73%)	500 mA h g <sup>-1</sup> @ 0.46 A g <sup>-1</sup>	5
CoMnFeO <sub>4</sub>	91.7 mA g <sup>-1</sup>	1448/1026	50 <sup>th</sup> (~68%)	600 mA h g <sup>-1</sup> @ 0.46 A g <sup>-1</sup>	6
(Ni <sub>0.2</sub> Co <sub>0.2</sub> Mn <sub>0.2</sub> Fe <sub>0.2</sub> Ti <sub>0.2</sub> ) <sub>3</sub> O <sub>4</sub>	100 mA g <sup>-1</sup>	900/560	100 <sup>th</sup> (~100%)	435 mA h g <sup>-1</sup> @ 0.5 A g <sup>-1</sup>	This work

**Table S3.** Lithiation/delithiation characteristics of conversion reaction spinel-structured transition metal oxide anodes.

Material	Lithiation products	Reduction potential (vs. Li <sup>+</sup> /Li)	Delithiation products	Oxidation potential (vs. Li <sup>+</sup> /Li)	Ref.
Mn <sub>3</sub> O <sub>4</sub>	Mn	0.2-0.4 V	Mn <sub>3</sub> O <sub>4</sub>	1.2-1.4 V	7 8
Fe <sub>3</sub> O <sub>4</sub>	Fe	0.8-1.0 V	FeO, Fe <sub>3</sub> O <sub>4</sub>	1.6-1.9 V	9 10
Co <sub>3</sub> O <sub>4</sub>	Co	0.9-1.4 V	CoO	2.0-2.3 V	11 12
CoMn <sub>2</sub> O <sub>4</sub>	Mn, Co	0.47 V, 1.25 V	MnO, CoO	1.44 V, 2.03 V	13 14
NiMn <sub>2</sub> O <sub>4</sub>	Mn, Ni	0.42 V, 1.13 V	Mn <sub>3</sub> O <sub>4</sub> , NiO	1.25 V, 1.96 V	15
MnFe <sub>2</sub> O <sub>4</sub>	Mn, Fe	0.76 V	MnO, Fe <sub>3</sub> O <sub>4</sub>	1.7 V	16 17
CoFe <sub>2</sub> O <sub>4</sub>	Co, Fe	0.75 V	CoO, Fe <sub>2</sub> O <sub>3</sub>	1.6-1.9 V	18
NiFe <sub>2</sub> O <sub>4</sub>	Fe, Ni	0.84 V, 0.98 V	NiO, Fe <sub>2</sub> O <sub>3</sub>	1.73 V, 2.12 V	16 19
MnCo <sub>2</sub> O <sub>4</sub>	Mn, Co	0.85 V	MnO, CoO	1.55 V, 2.05 V	20
FeCo <sub>2</sub> O <sub>4</sub>	Fe, Co	0.72 V, 1.57 V	FeO, Co <sub>3</sub> O <sub>4</sub>	1.69 V, 2.2 V	21 22
NiCo <sub>2</sub> O <sub>4</sub>	Ni, Co	0.81-1.25 V	NiO, Co <sub>3</sub> O <sub>4</sub>	1.5 V, 2.27 V	23 24

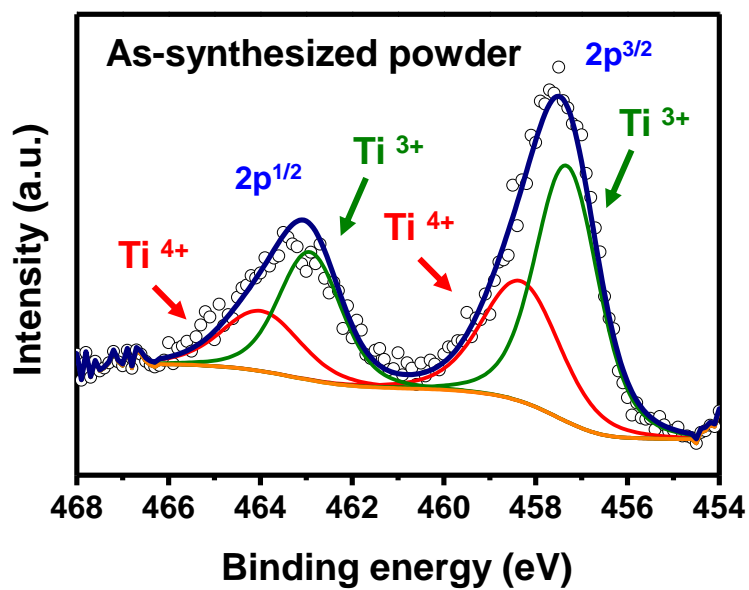
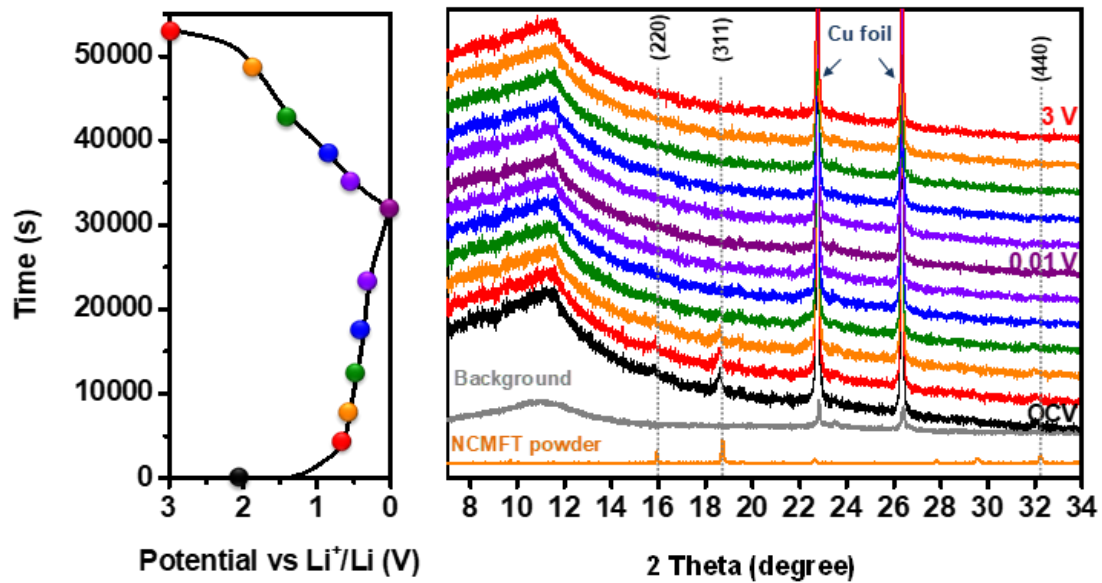


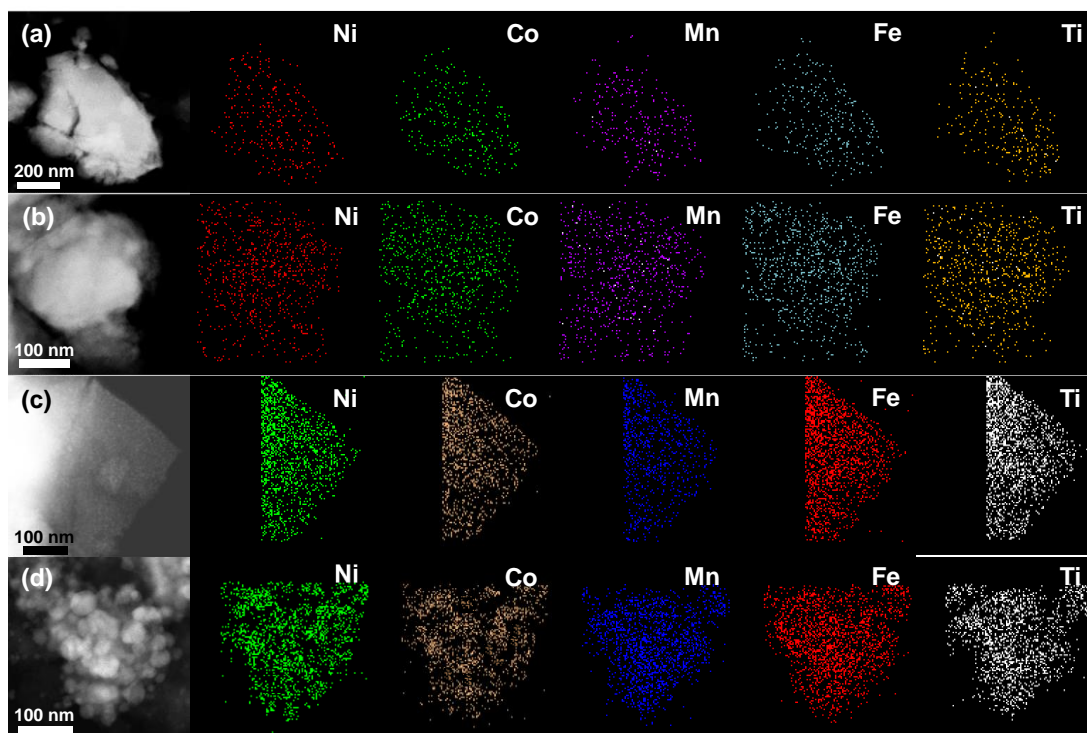
Figure S5. Ti 2p XPS spectrum of as-synthesized NCMFT powder

Table S4. The estimated positive charges of as-synthesized NCMFT powder and NCMFT electrode at OCV.

	as-synthesized Powder	Electrode at OCV
Ni	2.4+	2.8+ (measured in a coin cell)
Co	2.4+	2.4+ (measured in a coin cell)
Mn	2.6+	2.6+ (measured in a coin cell)
Fe	2.9+	2.4+ (measured in a coin cell)
Ti	3.4+	3.9+ (as-prepared electrode)
Total positive charges	8.2+	8.5+



**Figure S6.** In operando synchrotron XRD patterns of the NCMFT anode.



**Figure S7.** STEM-EDS analysis of NCMFT: (a) the 1<sup>st</sup> lithiation; (b) the 1<sup>st</sup> delithiation; (c) the 10<sup>th</sup> lithiation; (d) the 10<sup>th</sup> delithiation. Images labeled as Ni, Co, Mn, Fe, and Ti are intensity maps for characteristic X-rays.

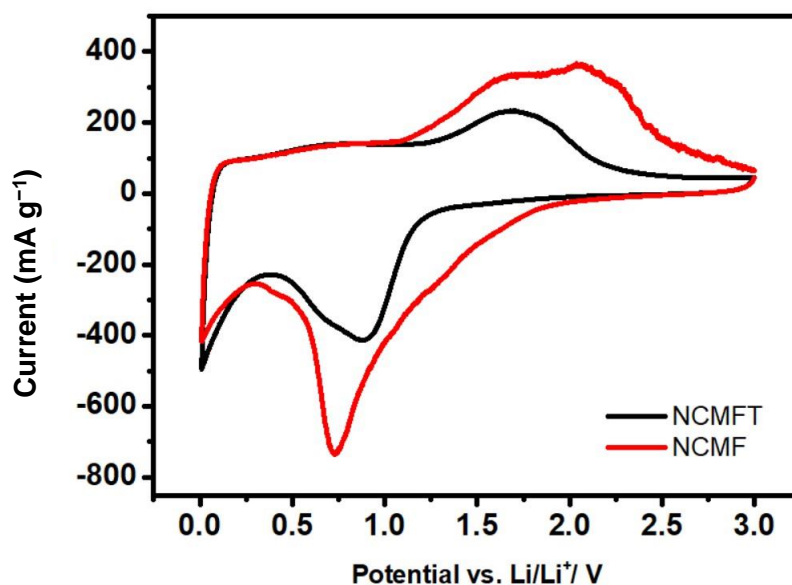


**Figure S8.** The CV curves of NCMFT and NCMF anodes in the 2<sup>nd</sup> cycle between 0.01 and 3.0 V vs. Li/Li<sup>+</sup> at a scan rate of 0.1 mV s<sup>-1</sup>

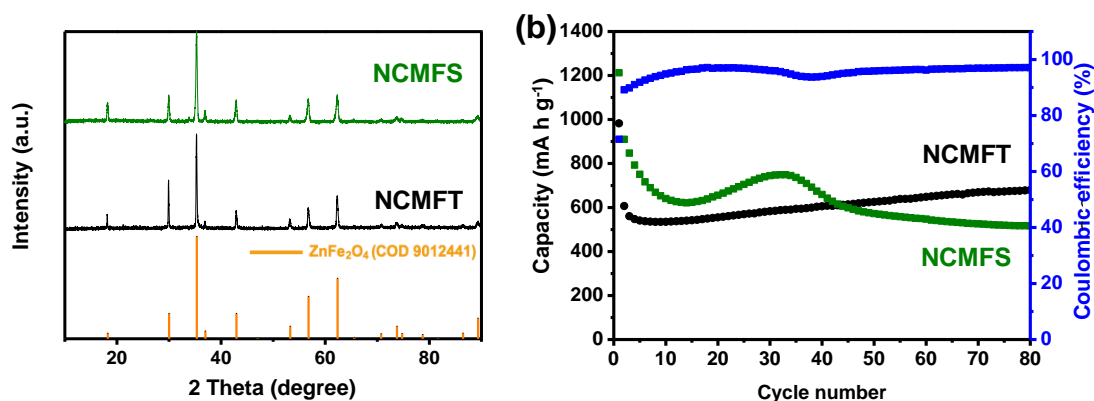


**Figure S9.** (a) XRD patterns of NCMFS and NCMFT. (b) The cycling performance of NCMFS and NCMFT anodes and the coulombic efficiency of NCMFS anode at current density of 50 mA g<sup>-1</sup>.

## Reference

1. H. Wang, L.-F. Cui, Y. Yang, H. Sanchez Casalongue, J. T. Robinson, Y. Liang, Y. Cui and H. Dai, *Journal of the American Chemical Society*, 2010, **132**, 13978-13980.
2. Z.-S. Wu, W. Ren, L. Wen, L. Gao, J. Zhao, Z. Chen, G. Zhou, F. Li and H.-M. Cheng, *ACS Nano*, 2010, **4**, 3187-3194.
3. H. Kim, J.-W. Lee, D. Byun and W. Choi, *Nanoscale*, 2018, **10**, 18949-18960.
4. Y. Zou, Z. Li, Y. Liu, J. Duan and B. Long, *Journal of Alloys and Compounds*, 2020, **820**, 153085.

5. S. Permien, A.-L. Hansen, J. van Dinter, S. Indris, G. Neubüser, L. Kienle, S. Doyle, S. Mangold and W. Bensch, *ACS Omega*, 2019, **4**, 2398-2409.
6. S. Permien, S. Indris, A.-L. Hansen, M. Scheuermann, D. Zahn, U. Schürmann, G. Neubüser, L. Kienle, E. Yegudin and W. Bensch, *ACS Applied Materials & Interfaces*, 2016, **8**, 15320-15332.
7. J. Gao, M. A. Lowe and H. D. Abruña, *Chemistry of Materials*, 2011, **23**, 3223-3227.
8. G. Jian, Y. Xu, L.-C. Lai, C. Wang and M. R. Zachariah, *Journal of Materials Chemistry A*, 2014, **2**, 4627-4632.
9. J.-Z. Wang, C. Zhong, D. Wexler, N. H. Idris, Z.-X. Wang, L.-Q. Chen and H.-K. Liu, *Chemistry – A European Journal*, 2011, **17**, 661-667.
10. Y. Wan, Z. Yang, G. Xiong and H. Luo, *Journal of Materials Chemistry A*, 2015, **3**, 15386-15393.
11. L. Luo, J. Wu, J. Xu and V. P. Dravid, *ACS Nano*, 2014, **8**, 11560-11566.
12. Q. Su, J. Zhang, Y. Wu and G. Du, *Nano Energy*, 2014, **9**, 264-272.
13. G. Yang, X. Xu, W. Yan, H. Yang and S. Ding, *Electrochimica Acta*, 2014, **137**, 462-469.
14. L. Zhou, D. Zhao and X. W. Lou, *Advanced Materials*, 2012, **24**, 745-748.
15. W. Kang, Y. Tang, W. Li, X. Yang, H. Xue, Q. Yang and C.-S. Lee, *Nanoscale*, 2015, **7**, 225-231.
16. N. Wang, X. Ma, Y. Wang, J. Yang and Y. Qian, *Journal of Materials Chemistry A*, 2015, **3**, 9550-9555.
17. S. Liu, J. Xie, Q. Su, G. Du, S. Zhang, G. Cao, T. Zhu and X. Zhao, *Nano Energy*, 2014, **8**, 84-94.
18. B. Wang, G. Wang, Z. Lv and H. Wang, *Physical Chemistry Chemical Physics*, 2015, **17**, 27109-27117.
19. P. Permude, S. Mohapatra, S. Nair, D. Santhanagopalan and D. A. Rai, *RSC Adv.*, 2016, **6**.
20. J. Li, S. Xiong, X. Li and Y. Qian, *Nanoscale*, 2013, **5**, 2045-2054.
21. S. G. Mohamed, C.-J. Chen, C. K. Chen, S.-F. Hu and R.-S. Liu, *ACS Applied Materials & Interfaces*, 2014, **6**, 22701-22708.
22. L. Liu, H. Zhang, Y. Mu, J. Yang and Y. Wang, *ACS Applied Materials & Interfaces*, 2016, **8**, 1351-1359.
23. G. Gao, H. B. Wu and X. W. Lou, *Advanced Energy Materials*, 2014, **4**, 1400422.
24. S. Abouali, M. Akbari Garakani, Z.-L. Xu and J.-K. Kim, *Carbon*, 2016, **102**, 262-272.